A density functional theory study of methyl shifts and methylcyclopropanol ion formation in $C_4H_8O^{+\cdot}$ ions

Charles E. Hudson, David J. McAdoo*

Marine Biomedical Institute, University of Texas Medical Branch, 301 University Boulevard, Galveston, TX 77555-1069, USA

Abstract

$C_4H_8O^{+\cdot}$ ions undergo a number of skeletal isomerizations, including rearrangement to the 2-butanone ion before metastable dissociation. However, the mechanisms whereby these rearrangements take place are not all firmly resolved. To remedy this, we characterized potential steps in the skeletal isomerizations of $C_4H_8O^{+\cdot}$ ions using density functional theory. We established that branched and straight chain $C_4H_8O^{+\cdot}$ ions with the oxygen on the terminal carbon interconvert through methylcyclopropanol ions and β-distonic ions. The cyclic isomers were found to be more stable than their ring-opened β-distonic forms. Transformation of ions with the O on a terminal carbon to ions with O on the second carbon occurs by methyl shifts that convert $CH_2CH(CH_3)CH=OH^+$ and $CH_3CH_2CH=CHOH^{+\cdot}$ to $CH_3CH(OH)CH=CH_2^{+\cdot}$. The second methyl shift takes place by inversion of the methyl configuration, possibly in accord with predictions of Woodward–Hoffmann rules. (Int J Mass Spectrom 199 (2000) 41–57) © 2000 Elsevier Science B.V.

Keywords: Alkyl shifts; Three-membered rings; Density functional theory; $C_4H_8O^{+\cdot}$

1. Introduction

We submit this work as a birthday greeting to Henri Audier on the occasion of his 60th birthday and in honor of his substantial body of work on related isomerizations in gas phase ion chemistry [1–3].
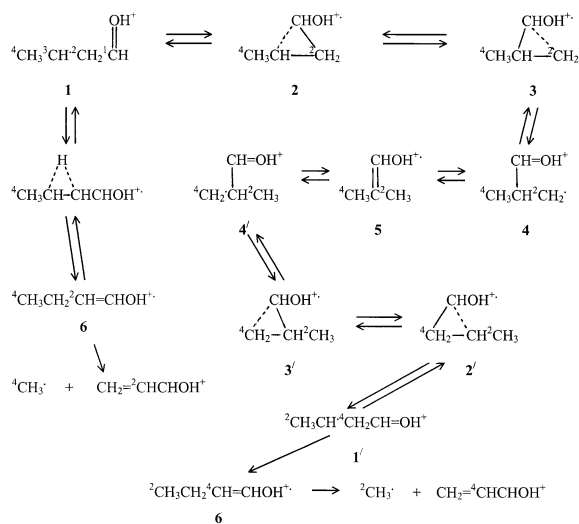
$C_nH_{2n}O^{+\cdot}$ and $C_nH_{2n}O_2^{+\cdot}$ species rearrange extensively [4–6]; at the extreme it has been proposed that approximately 60 $C_5H_{10}O^{+\cdot}$ isomers access each other [7]. However, these extensive isomerizations can be accounted for by combinations of a relatively small set of simple elementary reactions that are common to $C_nH_{2n}O^{+\cdot}$ and $C_nH_{2n}O_2^{+\cdot}$ ions [8]. These reactions include three-membered-ring shifts of hydrogens, functional groups, and alkyl groups. Three-membered-ring H transfers vary from being very facile to having high barriers in organic intermediates, depending on the occupancy of the orbitals into which the electron(s) associated with the H must go in the transition state [9–11]. The same considerations apply to 1,2 shifts of alkyl groups. We used density functional theory (DFT) to characterize 1,2-methyl shifts in $C_4H_8O^{+\cdot}$ isomers because it has been suggested that such shifts produce the skeletal isomerizations of $C_4H_8O^{+\cdot}$ ions, and because alkyl shifts are not well characterized in gas phase ion chemistry.

Near threshold, branched and straight chain $C_4H_8O^{+\cdot}$ ions with the oxygen on the first carbon (C1

Scheme 1.

ions) interconvert prior to decomposing [12,13]. $CH_3CH=CHOH^{+\cdot} \rightarrow CH_2^{\cdot}CH_2CH=OH^+$ [5,6,14–19] illustrates a generally important 1,2 H shift in $C_nH_{2n}O^{+\cdot}$ ions. The analogous methyl shift $CH_3CH_2CH=CHOH^{+\cdot} \rightarrow CH_2^{\cdot}CH(CH_3)CH=OH^+$ might therefore contribute to the interconversion of straight and branched chain $C_4H_8O^{+\cdot}$ isomers. However, ^{13}C labeling has demonstrated that this reaction does not occur [13]. An alternative pathway through ionized methylcyclopropanols for interconverting branched and straight chain C1 isomers is given in Scheme 1. This pathway is consistent with ^{13}C labeling results [13]. It is also otherwise plausible because skeletal rearrangements through ionized substituted cyclopropanes are widespread [20–23]. Although it is not established, the pathway in Scheme 1 is probably the one that interconverts branched and straight chain C1 ions, given the lack of reasonable alternatives. Carbons are numbered throughout as is **1** in Scheme 1.
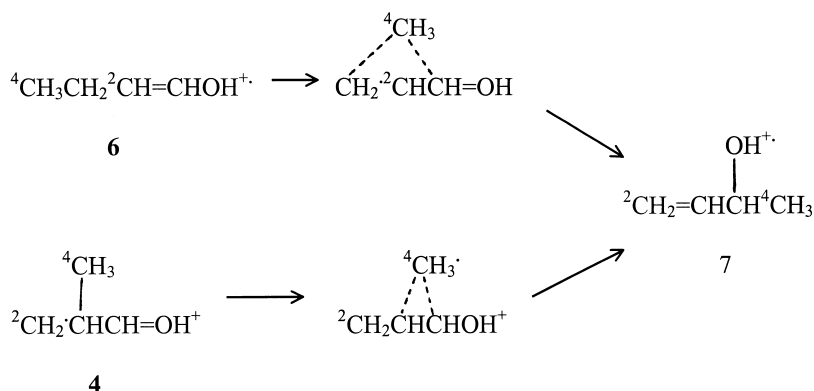
In 1979 we proposed that near their thresholds for dissociation many $C_4H_8O^{+\cdot}$ C1 ions isomerize to structures with the oxygen on the second carbon (C2 ions) and decompose through the 2-butanone ion [12]. This interpretation was devised to explain complementary labeling patterns in the methyls and ethyls lost from deuterated C1 isomers, as that pattern characterizes dissociation through the 2-butanone rad-

ical cation [17]. Oxygen also shifts from the first to the middle position in some metastable $C_5H_{10}O^{+\cdot}$ isomers [24,25], undoubtedly by mechanisms similar to the C1–C2 transformation in $C_4H_8O^{+\cdot}$ ions. However, the steps by which oxygens are relocated have not been clearly defined, and whether such relocation occurs in $C_4H_8O^{+\cdot}$ C1 ions has even been questioned [26] on the grounds that $CH_2=CHCHOH^+$ rather than $CH_3CH_2CO^+$ is formed by methyl loss from those ions. However, a mixture of $CH_3CH_2CO^+$ and $CH_2=CHCH=OH^+$ is actually formed by methyl loss from C1 ions, demonstrating dissociations with and without isomerization to C2 structures [27]. The exclusive formation of CH_3CO^+ by loss of ethyl from $C_4H_8O^{+\cdot}$ isomers confirms that some C1 ions decompose through $CH_3C(=O^{+\cdot})CH_2CH_3$, as there is no reasonable way for C1 ions to dissociate directly to CH_3CO^+ [27].

The C1 → C2 conversion was initially attributed to 1,2 and 1,3 shifts of the hydroxyl group [12]. However, even though a 1,3-hydroxyl shift was indicated to be plausible by early MINDO/3 calculations [28], the dissociation pattern of $CH_3CH=CH^{13}CH_2OH^{+\cdot}$ eliminated that possibility [13]. Contrary to predictions for OH shifts, there was no ^{13}C in either the methyl or ethyl lost from this ion. Recent ab initio studies [16] place the high point in the 1,3-OH shift in $CH_2=CHCH_2OH^{+\cdot}$ 76 kJ mol^{-1} above the critical energy for $CH_2^{\cdot}CH_2CH=OH^+ \rightarrow CH_2=CHCH_2OH^{+\cdot}$, a reaction similar to **4 → 7**. This provides additional evidence that 1,3 OH shifts are not competitive with other available isomerizations in $C_nH_{2n}O^{+\cdot}$ species. $C_3H_6O^{+\cdot}$ isomers with the oxygen on the first and second carbons do not interconvert, even at high internal energies [29,30], further demonstrating that 1,2-O shifts do not occur.

The obvious remaining ways to change the location of the oxygen together with the C that bears it in the carbon skeleton are the 1,2 and 1,3 methyl shifts illustrated in Scheme 1 and pathways through ionized methylcyclopropanols as illustrated in Scheme 3.

The ring in the first structure in Scheme 1 might open in three ways, with the opening required to shift the O to the second position probably being the highest in energy. That reaction is therefore unlikely

$$^4CH_3CH_2{}^2CH=CHOH^{+\cdot} \longrightarrow \overset{\overset{\displaystyle ^4CH_3}{\diagup\;\vdots\;\diagdown}}{\dot{C}H_2 \cdots {}^2\dot{C}HCH=OH}$$

6

$$^2CH_2=CHCH{}^4CH_3 \quad \text{(with } OH^{+\cdot} \text{ above)}$$

$$\overset{\overset{\displaystyle ^4CH_3}{|}}{{}^2CH_2\dot{C}HCH=OH^+} \longrightarrow {}^2CH_2\dot{C}HCHOH^+ \; (\text{with } {}^4CH_3\cdot \text{ above})$$

4

7

Scheme 2.

to be competitive with the ring openings in Scheme 1, predicting that the pathway in Scheme 2 is not important. The 1,2-methyl shift in Scheme 1 is the most likely step transforming C1 to C2 ions [13,31], despite appearance energies suggesting a slightly higher threshold for forming CH_3CO^+ from **7** than from C1 ions [32].

To define better the isomerizations of $C_nH_{2n}O^{+\cdot}$ ions and add to our understanding of what determines the pathways taken in these reactions, we characterized the skeletal isomerizations in Schemes 1–3 by density functional theory.
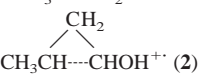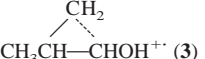
2. Theory

Calculations were carried out using B3LYP hybrid density functional/self consistent field theory [33,34]

using a 6-31G(d) basis set (here abbreviated DFT) as implemented in the Gaussian 94 suite of programs [35] on a Cobra Carrera Alpha computer. DFT was used because it is faster than quadratic configuration interaction procedures and typically gives reasonably accurate ion energies [36]. Structures other than those for trans **6** and trans **8** were determined using the opt=tight criterion in Gaussian 94. Exact optima for trans **6** and trans **8** could not be satisfactorily located with this routine because of difficulties in optimizing dihedral angles to the high tolerances in opt=tight. Zero point energies were determined by multiplying the frequencies obtained by theory by 0.9806 [37]. Intrinsic reaction coordinate (IRC) calculations [38,39] were sometimes carried out to verify that particular transition states connected the desired potential minima and in some instances to trace the motions of atoms from reactants to products.
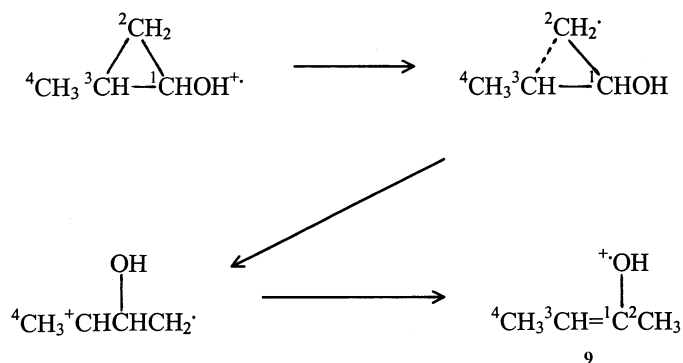
Scheme 3.

Table 1
Density functional theory {B3LYP/6-31G(d)} energies for $C_4H_8O^{+\cdot}$ species

Ion	Theory (Hartrees)	ZPE (kJ mol^{-1})	Theory (kJ mol^{-1})	Experiment (kJ mol^{-1})
t-CH$_3$CH$^\cdot$CH$_2$CH=OH$^+$ (**1**)	−232.110958	286.7	70.9	
$\overset{\displaystyle CH_2}{CH_3CH\text{---}CHOH^{+\cdot}}$ (**2**)	−232.125419	290.4	36.6	
$\overset{\displaystyle CH_2}{CH_3CH\text{—}CHOH^{+\cdot}}$ (**3**)	−232.114606	289.9	64.5	
t-CH$_3$CH(CH$_2$)CH=OH$^+$ (**4**)	−232.101005	285.4	95.7	
c-CH$_3$CH(CH$_2$)CH=OH$^+$ (**4**)	−232.103518	286.9	90.6	
t-CH$_3$CH$_2$CH=CHOH$^{+\cdot}$ (**6**)	−232.140420	292.7	0	628
c-CH$_3$CH$_2$CH=CHOH$^{+\cdot}$ (**6**)	−232.140244	293.2	1.0	
CH$_3$CHOHCH=CH$_2^{+\cdot}$ (**7**)	−232.097995	286.1	104.3	756
c-CH$_3$C(=O$^+$)CH$_2$CH$_3$ (**8**)	−232.132634	284.1	11.4	677
t-CH$_3$C(=O$^+$)CH$_2$CH$_3$ (**8**)	−232.133603	285.3	10.0	
t-TS(**1** → **2**)	−232.105406	286.0	84.8	
t-TS(**2** → **3**)	−232.113604	289.5	66.7	
t-TS(**3** → **4**)	−232.097541	286.1	105.5	
c-TS(**3** → **4**)	−232.097745	286.7	105.6	
TS(**4** → **7**)	−232.085666	284.6	135.2	
TS(**6** → **1**)	−232.101161	280.9	91.3	
TS(**6** → **2**)	−232.096920	279.6	101.1	
t-TS(**6** → **4**)	−232.073863	274.3	155.9	
t-TS(**6** → **7**)	−232.074902	274.2	153.1	
c-TS(**6** → **7**)	−232.073769	274.3	156.1	
t-CH$_2$=CHCHOH$^+$	−192.233499	193.5		642
CH$_3^\cdot$	−39.838292	76.8		146
CH$_2$=CHCHOH$^+$ + CH$_3^\cdot$	−232.071791	270.3	157.3	788

Species preceded by t have the H on O oriented away from the rest of the molecule; those preceded by a c have that H oriented toward the rest of the molecule.

3. Results and discussion

Energies obtained for $C_4H_8O^{+\cdot}$ species and for the transition states for their skeletal isomerizations at the B3LYP/6-31G(d) level of DFT theory are given in Table 1. Potential energy diagrams summarizing our results are given in Figs. 1 and 2.

3.1. Structures

3.1.1. CH$_3$CH$^\cdot$CH$_2$CH=OH$^+$ (1)

The optimum structure for the straight chain β distonic ion CH$_3$CH$^\cdot$CH$_2$CH=OH$^+$ has its carbon chain extended, but with O and ^{3}C near rather than turned away from each other (Fig. 3). The distonic carbon is 2.501 Å from the oxygen-bearing carbon, so

this species is acyclic. The H on O, the O, ^{1}C, ^{2}C, ^{3}C, and the H on ^{1}C are all nearly in a plane (dihedral angles: HO^{1}C^{2}C 180.0°, ^{3}C^{2}C^{1}CO 0.0°, and ^{3}C^{2}C^{1}CH 180°). This largely reflects a necessity for atoms fully bonded to O and ^{1}C to all be in the same plane due to the π bond between these two atoms. The residence of ^{3}C in this plane suggests an attraction between that atom and oxygen, as this minimizes the distances between those two atoms, or it may simply result from staggering of hydrogens on adjacent carbons. Attempts to locate a structure for **1** with the O turned away from ^{3}C rather than toward it led only to cyclization to the methylcyclopropanol ion **2**. Inclusion of zero point energies placed **1** 70.9 kJ mol^{-1} above **6**, the latter being the lowest point on the portion of the $C_4H_8O^{+\cdot}$ potential energy surface explored.
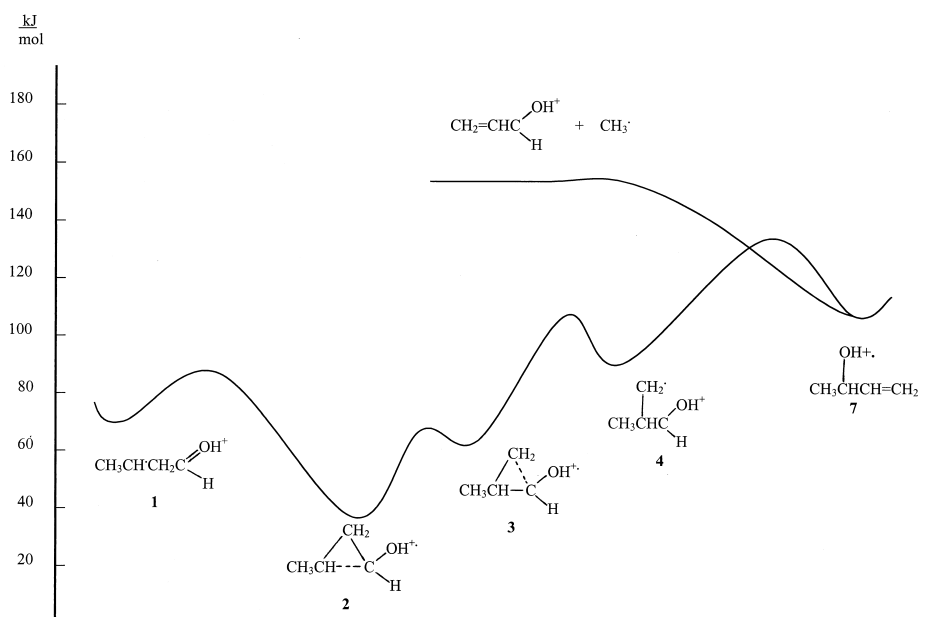
Fig. 1. Potential energy diagram for reactions of distonic and cyclic $C_4H_8O^{+\cdot}$ ions derived from the results of density functional theory.
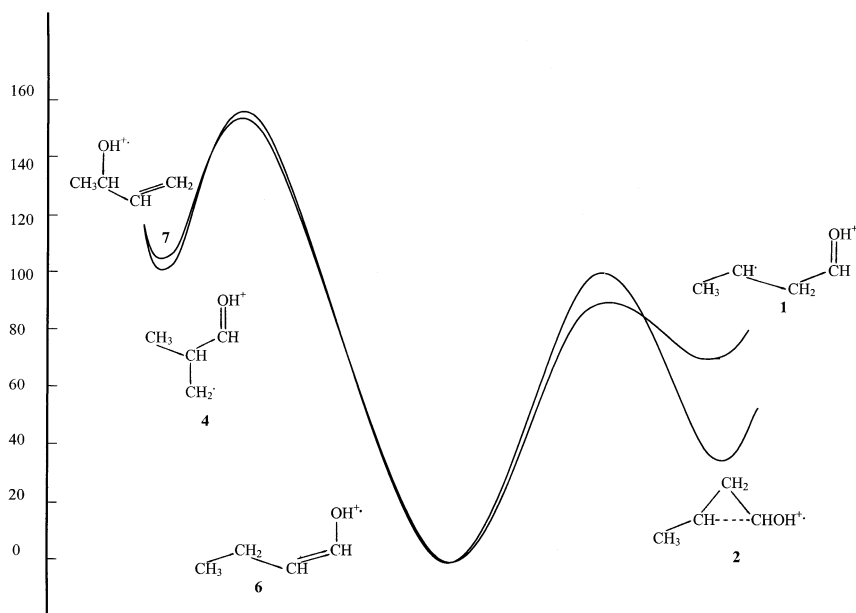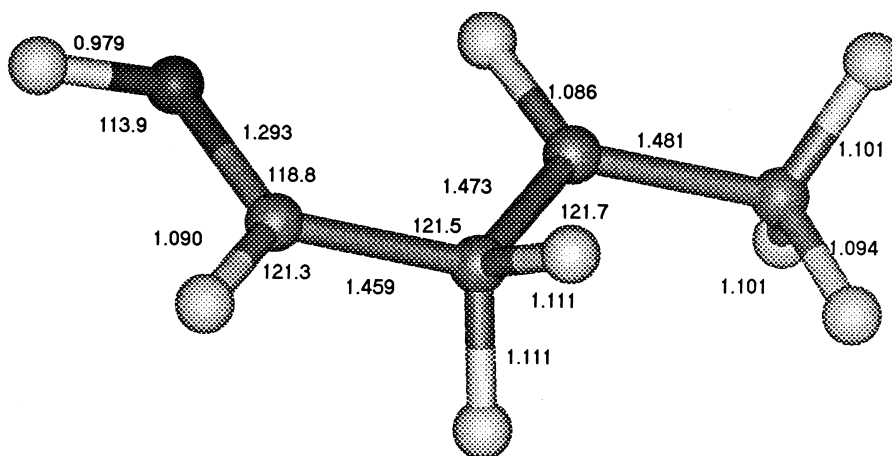
Fig. 2. Potential energy diagram according to DFT for isomerizations to and from $CH_3CH_2CH=CHOH^{+\cdot}$ (**6**).

Fig. 3. Geometry for **1** obtained by DFT.

3.1.2. $CH_3CH(CH_2)CH=OH^+$ (4)

The optimized structure found for the other β-distonic ion $CH_3CH(CH_2)CH=OH^+$ also had its O turned toward its distonic carbon (O–C = 2.805 Å) (Fig. 4), although an optimum with the oxygen away from this carbon was not sought for **4**. As in **1**, the

HOCHCC atoms were nearly in a plane (dihedral angles with HO trans: HO^{1}C^{3}C 182.0°, ^{2}C^{3}C^{1}CO −0.6°, and ^{2}C^{3}C^{1}CH −178.8°). Also as in **1**, the distonic C was far (2.515 Å) from the oxygen-bearing carbon. The most stable isomer of **4** found (H on O cis to the ^{2}C^{3}C bond) is 90.6 kJ mol^{-1} higher in energy
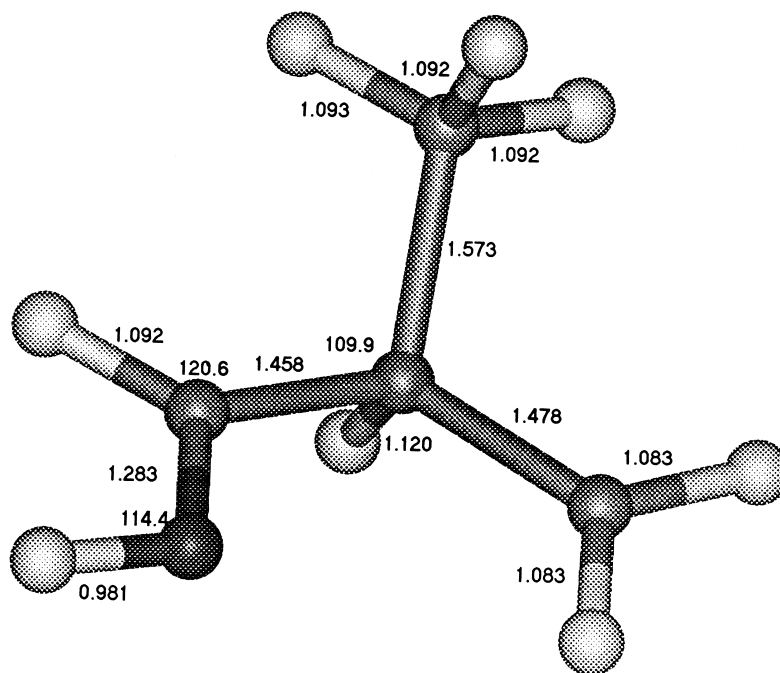
Fig. 4. Geometry for **4** obtained by DFT.
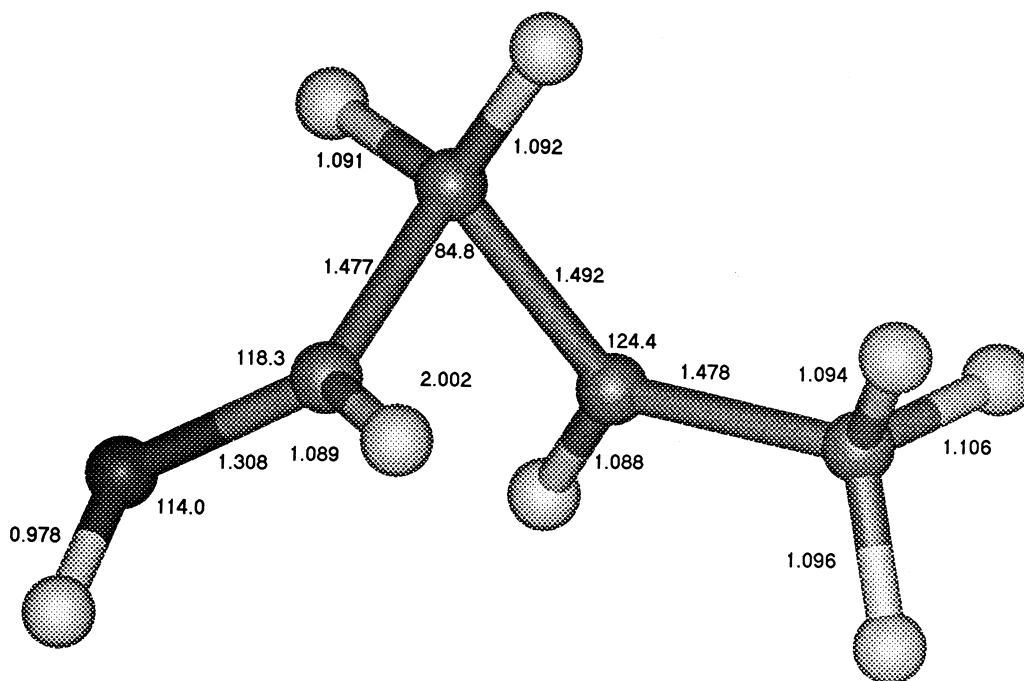
Fig. 5. Geometry for **2** obtained by DFT.

than **6** and 19.7 kJ mol^{-1} above **1**, the other β-distonic species.

3.1.3. CH$_3$($\overline{CH}$)CH$_2$($\overline{CH}$)OH$^{+\cdot}$ (2)

Similar to findings by Bouchoux and co-workers regarding ionized cyclopropanol [16], **2** (Fig. 5) represents a potential minimum only 36.6 kJ mol^{-1} higher in energy than **6**. Structure **2** is 34 kJ mol^{-1} more stable than the related open configuration **1**, so cyclic C$_4$H$_8$O$^{+\cdot}$ configurations are more stable than the corresponding β-distonic ones. The ^{1}C–^{3}C bond is 2.002 Å long, about 0.5 Å longer than CC single bonds in C$_4$H$_8$O$^{+\cdot}$ ions, but much shorter than the 2.501 Å in **1**. Even though the C–C bond is elongated, this configuration and an overlap density of 0.115 between ^{1}C and ^{3}C (as compared to 0.740 in ^{3}C–^{4}C) suggest bonding. The presence of appreciable electron density between ^{1}C and ^{3}C, its stability, orientation of substituents, and a ^{3}C^{2}C^{1}C bond angle of 84.8° versus a corresponding angle of 114° in **1** demonstrate that **2** can be regarded as a methylcyclopropanol ion (bond angles smaller than 90° are always in small rings in

organic chemistry). The CO bond is 98° out of the plane of the ^{3}C^{2}C^{1}C ring and the CH bond at the same carbon is at 83° to the plane on the opposite side. Thus the planarity of ^{3}C with the protonated carbonyl substituents observed in **1** and **4** is disrupted in **2**. However, C–O and all of the atoms attached to them are nearly planar (dihedral angles HOCH = −6.5° and HOCC = 174.4°), despite formation of a weak bond between ^{3}C and ^{1}C.

3.1.4. CH$_3$($\overline{CH}$)CH$_2$–($\overline{CH}$)OH$^{+\cdot}$ (3)

This bond (Fig. 6) is very similar in properties to **2** according to DFT, except that the ^{1}C–^{3}C bond was of normal length (1.487 Å) and the ^{1}C–^{2}C bond was lengthened to 1.924 Å. Similarly to **2**, there was appreciable overlap electron density—0.085—between ^{1}C and ^{2}C, so **3** can be considered a second long-bonded methylcyclopropanol isomer. This is confirmed by a ^{1}C^{3}C^{2}C bond angle of 80.7° versus a corresponding angle of 117.9° in **4**. Again the H and O attached to ^{1}C are above and below the plane of the ring (dihedral angles: ^{2}C^{3}C^{1}CO −97.8°, ^{2}C^{3}C^{1}CH
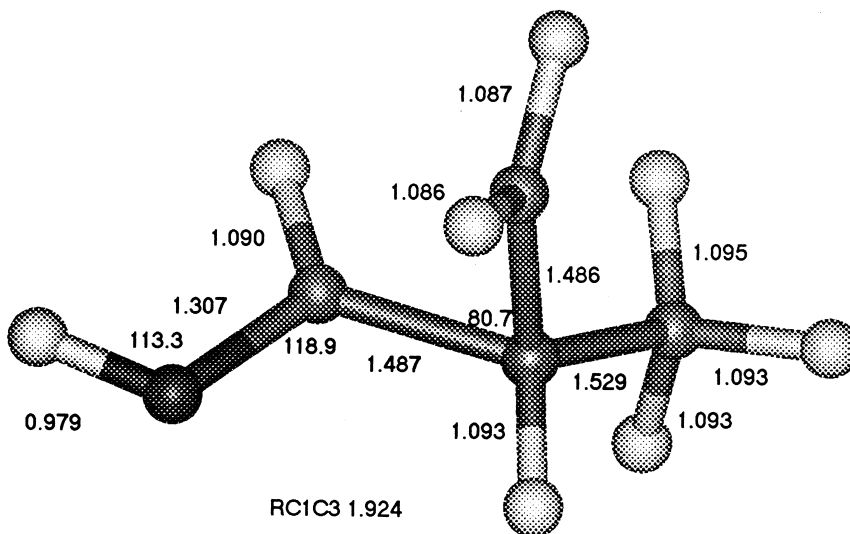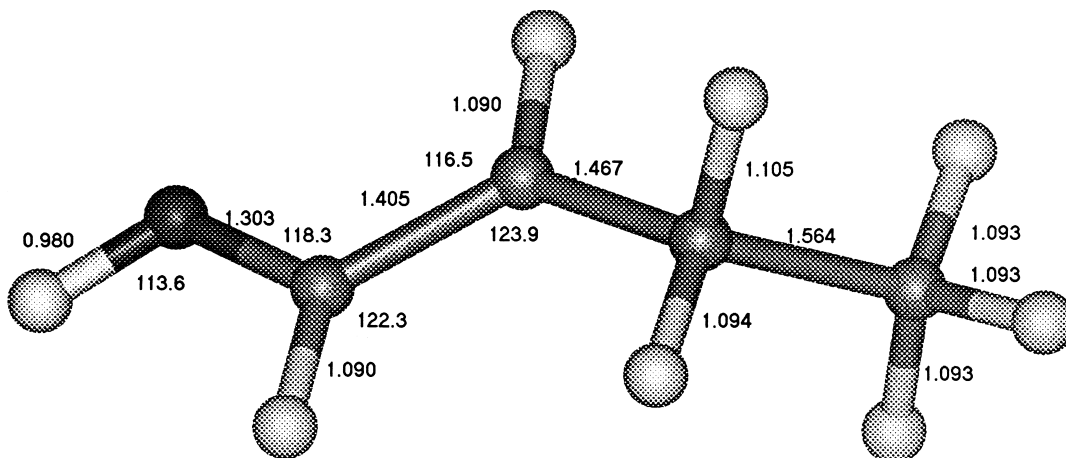
Fig. 6. Geometry for **3** obtained by DFT.

85.6°), and the distant carbon in the long bond is out of the protonated carbonyl plane. As in **1** versus **2**, **3** is more stable (26–31 kJ mol^{-1}) than its acyclic form **4**.

3.1.5. CH$_3$CH$_2$CH=CHOH$^{+\cdot}$ (6)

This bond is the most stable C1 ion examined and was used as the reference zero point for the C$_4$H$_8$O$^{+\cdot}$ potential surface. **6** was fully extended in its equilibrium geometry with approximately normal length CC

bonds (Fig. 7). The ^{1}C–^{2}C bond was slightly shortened (1.405 Å) and the ^{3}C–^{4}C bond (1.564 Å) slightly extended relative to the ^{2}C–^{3}C bond (1.467 Å). The first suggests some double bond character. The structure of **6** was optimized according to the standard criteria, but not the more stringent opt=tight criteria. Optimization according to the latter criteria could not be achieved, despite considerable effort. The nonoptimized displacements were for torsional modes. We consider the energy of trans-**6** to be accurate because

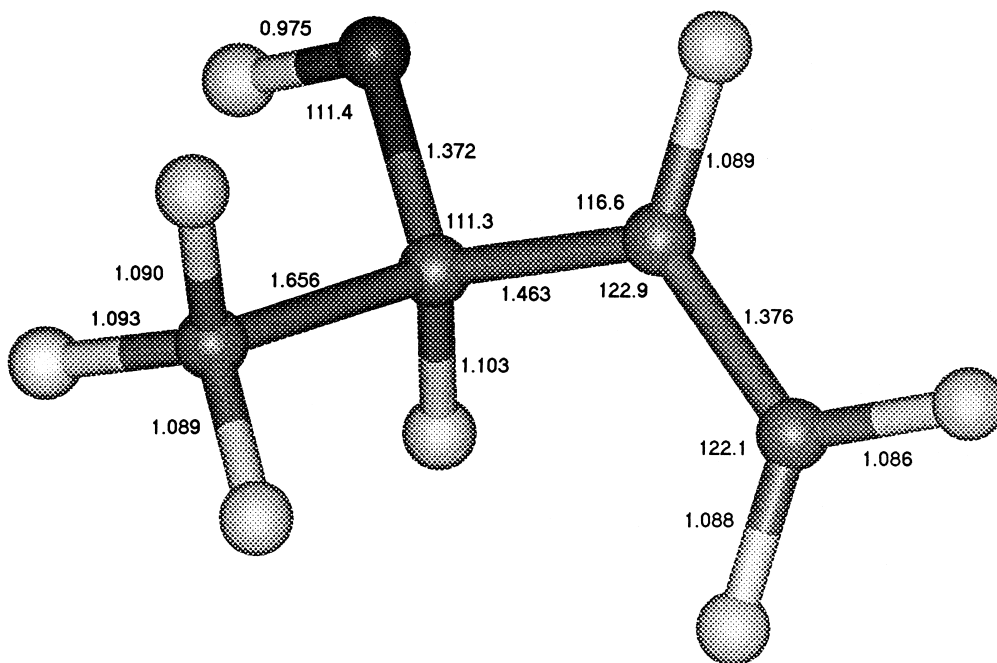Fig. 7. Geometry for **6** obtained by DFT.

Fig. 8. Geometry for **7** obtained by DFT.

energies obtained for structures within the near vicinity of that chosen were within 0.1 kJ mol^{-1} of that reported.

3.1.6. $CH_3CHOHCH=CH_2^{+\cdot}$ (7)

This bond has an unusual feature—its CC bond to methyl was 1.656 Å long, about 0.1 Å longer than a normal single C–C bond (Fig. 8). Its ^3C–^4C bond (1.376 Å) was shortened relative to its ^3C–^2C bond (1.463 Å), indicating double bond character in the former, although it is still about 0.06 Å longer than a typical CC double bond. The C–O bond length (1.372 Å) was also slightly longer than in the other species examined here (1.265 Å in **1** to 1.308 Å in **2**), reflecting some C–O double bond character in the latter ions. In light of the lengthened ^1C–^2C distance, we calculated spin and charge densities at each heavy atom to determine how close **7** may be to a methyl-protonated acrolein complex. The Mulliken charge densities condensed to the heavy atoms were O -0.04, ^1C 0.24, ^2C 0.28, ^3C 0.25, and ^4C 0.27; the corresponding spin densities were 0.18, 0.19, 0.04, 0.14 and 0.45. The high spin density at ^4C suggests

that the methyl attached by the lengthened bond has some of the character of a free methyl group. However, the protonated acrolein portion of **7** is nonplanar about the carbon bearing the O, so **7** is not a methyl radical-protonated acrolein ion–neutral complex. In energy, **7** is the highest energy stable $C_4H_8O^{+\cdot}$ isomer examined, 104.3 kJ mol^{-1} above **6**.

3.1.7. $CH_3C(=O^{+\cdot})CH_2CH_3$ (8)

This bond was included in present calculations primarily to provide an additional calibration point on the energy scale. Two structures were found, one with its ^4C methyl gauche to the oxygen and one with its ^4C methyl oriented away from the oxygen (Fig. 9). These two structures differed by only 1.4 kJ mol^{-1} in energy. The structure of **8** was otherwise without unusual features. According to the calculations, this ion is 10.0–11.4 kJ mol^{-1} above **6**, whereas the experimental difference is 49 kJ mol^{-1}. This suggests uncertainties in our DFT results as large as 40 kJ mol^{-1}, although some of the difference may also reflect inaccuracies in experimental values. Other differences between DFT values were closer to the
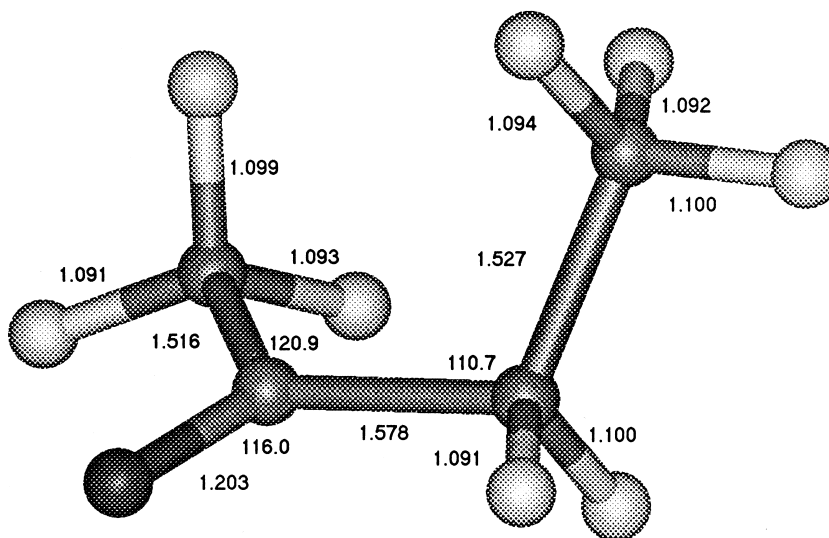
Fig. 9. Geometry for **8** obtained by DFT.

differences between experimental values. Theory places $\Delta_f H(\mathbf{7})$ 104.3 kJ mol^{-1} higher than $\Delta_f H(\mathbf{6})$, agreeing reasonably with an experimental difference of 128 kJ mol^{-1}. Assuming no reverse barrier to the dissociation, formation of CH$_2$=CHCHOH$^+$ + CH$_3^{\cdot}$ from **6** was predicted by theory to require 157.3 kJ mol^{-1}. This agrees quite well with a thermochemical difference of 160 kJ mol^{-1} and a difference of 167 kJ mol^{-1} based on a threshold for methyl loss of 795 kJ mol^{-1} derived from a photoionization appearance energy [32]. The mechanistic conclusions based on the present theoretical results are likely to be correct, as agreement between theory and experiment is reasonable for comparisons that can be made for species that are actually involved in the reactions studied here.

3.2. Interconversion of branched and straight-chain C1 ions—$\mathbf{1} \rightleftarrows \mathbf{2} \rightleftarrows \mathbf{3} \rightleftarrows \mathbf{4}$

3.2.1. $\mathbf{2} \rightleftarrows \mathbf{3}$

The lowest energy pathway found by DFT for interconverting branched and straight chain C1 ions was $\mathbf{1} \rightleftarrows \mathbf{2} \rightleftarrows \mathbf{3} \rightleftarrows \mathbf{4}$, resolving at last how that process occurs. Tracing the transformation of **2** to **3** by an intrinsic reaction coordinate (IRC) calculation

confirmed that the transition state assigned to that process (Fig. 10) was that for $\mathbf{2} \rightarrow \mathbf{3}$. Thus interconversion of the two low energy methylcyclopropanol ions **2** and **3** is the step that connects the branched and straight chain C1 C$_4$H$_8$O$^{+\cdot}$ isomers. The transition state for interchanging the two cyclic configurations was located only 2.2 kJ mol^{-1} above $\Delta_f H$ for **3**, the higher energy cyclic C$_4$H$_8$O$^{+\cdot}$ isomer, and somewhat below $\Delta_f H$ for the open isomers **1** and **4**. The critical energy for the analogous degenerate interconversion of "cyclopropanol" ions is also very low, only 5 kJ mol^{-1} [16]. Isomerization of the ring $\mathbf{2} \rightleftarrows \mathbf{3}$ involves shortening of the long ring C–C bond and lengthening of the ring C–C bond that becomes the long bond without much additional change in geometry. It also involves some twisting such that the distant carbon in the shortening bond moves into the plane of the protonated carbonyl group while the corresponding carbon in the lengthening bond moves out of that plane.

Although the branched and straight chain C1 isomers are actually interconverted by $\mathbf{2} \rightleftarrows \mathbf{3}$, $\Delta_f H(\mathbf{1})$ and $\Delta_f H(\mathbf{4})$ and the energies of the transition states (TS) connecting **1** to **2** and **4** to **3** are all above TS($\mathbf{2} \rightarrow \mathbf{3}$). The ring-opening–closing $\mathbf{3} \rightleftarrows \mathbf{4}$ probably has more influence than $\mathbf{2} \rightleftarrows \mathbf{3}$ on the rate of interconver-
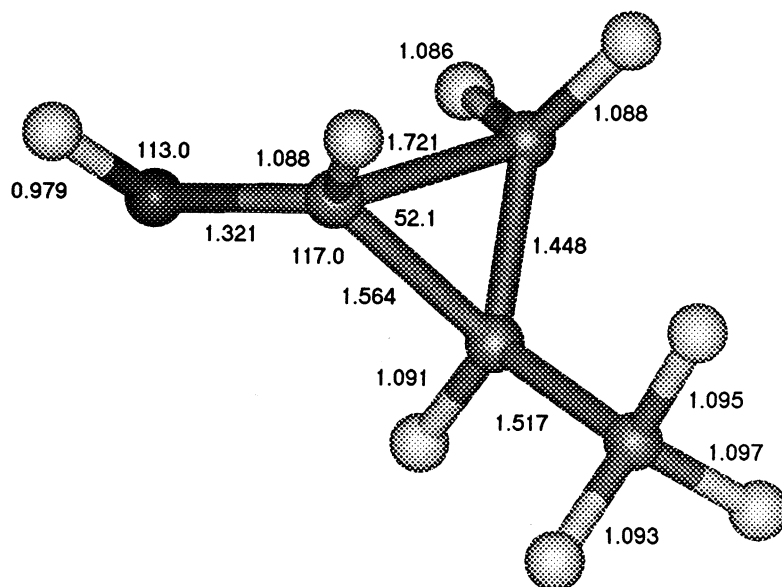
Fig. 10. Geometry for TS($\mathbf{2} \to \mathbf{3}$) obtained by DFT.

sion of branched and straight chain $C_4H_8O^{+\cdot}$ isomers, as $\mathbf{3} \rightleftarrows \mathbf{4}$ has the highest critical energy of the steps in that pathway. The barrier to $\mathbf{2} \to \mathbf{3}$ is about 68 kJ mol^{-1} below the transition state for converting C1 to C2 ions (see below), and about 91 kJ mol^{-1} below the threshold for dissociation to $CH_3^{\cdot}$ + CH_2=CHCH=OH$^+$; therefore $\mathbf{2} \to \mathbf{3}$ should be facile even below the thresholds for dissociation. Given the low barrier for converting $\mathbf{2}$ to $\mathbf{3}$ and the greater stability of $\mathbf{2}$, $\mathbf{2}$ would be the dominant species in a mixture of the two.

3.2.2. $\mathbf{1} \rightleftarrows \mathbf{2}$

To characterize further the interconversion of the distonic and cyclic $C_4H_8O^{+\cdot}$ isomers, the pathway from $\mathbf{1}$ to $\mathbf{2}$ was also traced by an IRC calculation, a calculation which verified that the transition state (Fig. 11) assigned to that process was correctly located. The $^3C^2C^1CO$ dihedral angle was 0.0° in $\mathbf{1}$, 36.4° at the transition state, and $-98.1°$ in the closed structure $\mathbf{2}$, and the values of the $^3C^2C^1CH$ dihedral angles were 180.0°, $-131.0°$, and 82.8° at the same points. Given that the difference between the dihedral angles was close to 180° throughout the course of the

reaction, the HO^{1}CH grouping remained close to planar all along the reaction coordinate. The $^1C^2C^3C$ angle varied from 114° in $\mathbf{1}$ to 80.7° in $\mathbf{2}$. However, the ^3C to O distance did not change very much (2.79 Å in $\mathbf{1}$ and 2.80 Å in $\mathbf{2}$). Thus the interconversion of $\mathbf{1}$ and $\mathbf{2}$ largely involves rotation of the HO^{1}CH between being planar with the $^1C^2C^3C$ triangle in $\mathbf{1}$ and being approximately perpendicular to it in $\mathbf{2}$, together with opening and closing of the $^1C^2C^3C$ angle. TS($\mathbf{1} \to \mathbf{2}$) is 84.8 kJ mol^{-1} higher in energy than $\mathbf{6}$ and 18 kJ mol^{-1} above TS($\mathbf{2} \rightleftarrows \mathbf{3}$).

3.2.3. $\mathbf{3} \rightleftarrows \mathbf{4}$

The transition state for the interconversion of $\mathbf{3}$ and $\mathbf{4}$ (Fig. 12) was located by the normal transition state finding routine. Similarly to $\mathbf{1} \rightleftarrows \mathbf{2}$, this reaction also involves the rotation of a nearly planar HO^{1}CH and opening and closing of the $^2C^3C^1C$ angle. For $\mathbf{4}$, TS($\mathbf{3} \rightleftarrows \mathbf{4}$) and $\mathbf{3}$, the $^2C^3C^1CO$ and $^2C^3C^1CH$ dihedral angles were, respectively, $-0.6°$ and 184°, 42.5° and $-178.8°$, and $-137.9°$ and 85.6°. Again the HO^{1}CH group remains planar while rotating. At 105.5 kJ mol^{-1} above $\mathbf{6}$, this transition state is the high point on the pathway interconverting $\mathbf{1}$ and $\mathbf{2}$.
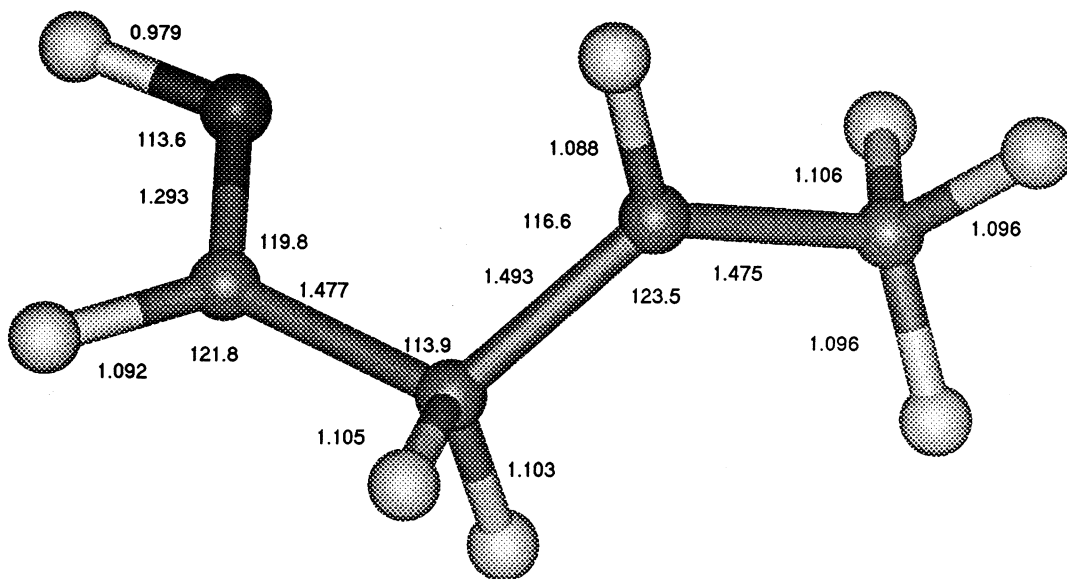
Fig. 11. Geometry for TS($\mathbf{1} \rightarrow \mathbf{2}$) obtained by DFT.
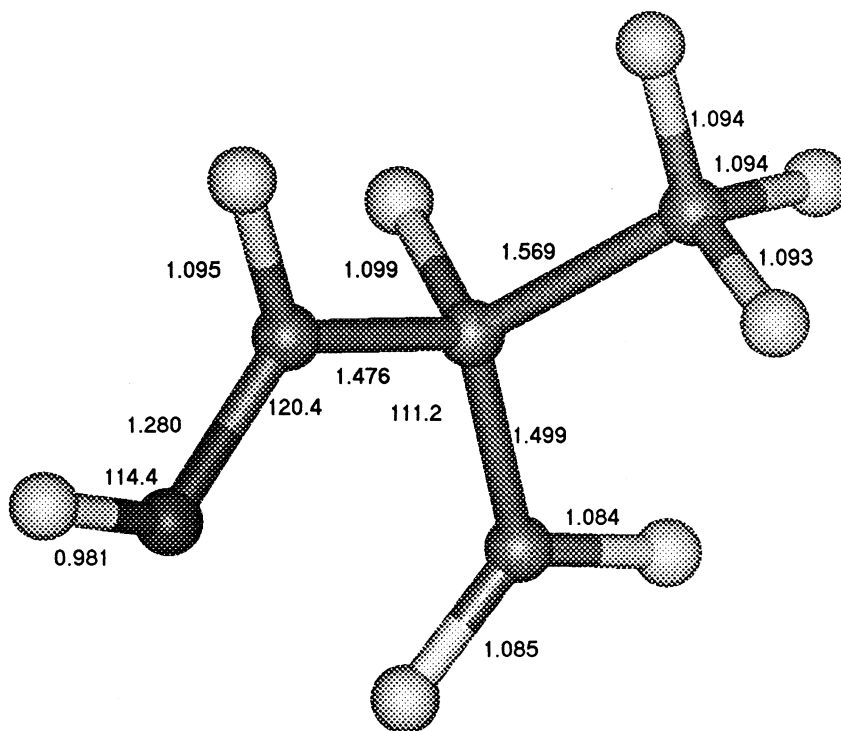
Fig. 12. Geometry for TS($\mathbf{3} \rightarrow \mathbf{4}$) obtained by DFT.
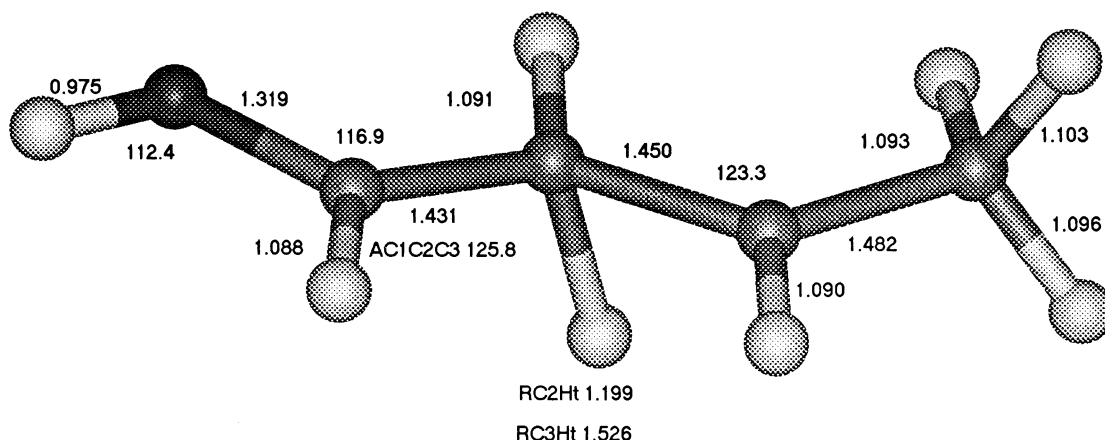
Fig. 13. Geometry for TS($\mathbf{6} \rightarrow \mathbf{2}$) obtained by DFT. H$t$ represents the H being transferred from ^{3}C to ^{2}C, and AC1C2C3 represents the ^{1}C^{2}C^{3}C angle. The figure depicts the transition state for $\mathbf{6} \rightarrow \mathbf{2}$ rather than that for $\mathbf{6} \rightarrow \mathbf{1}$ because OCCC is in a trans geometry; the reaction will therefore continue to $\mathbf{2}$.

3.2.4. $6 \rightleftarrows 1$ and $6 \rightleftarrows 2$

The transition states for the interconversions of $\mathbf{6}$ and $\mathbf{1}$ or $\mathbf{2}$ (Fig. 13) were located to characterize the interconversion of the enol and the distonic ions. A potential energy diagram for the isomerizations of $\mathbf{6}$ is given in Fig. 2. Given that $\mathbf{1}$ is only stable when the configurations of CCCO are cis and that trans-$\mathbf{1}$ spontaneously goes on to $\mathbf{2}$, the H-transfer transition states in the corresponding geometries connect $\mathbf{6}$ to $\mathbf{1}$ or $\mathbf{2}$. Consequently, we characterized transition states for H-transfer with CCCO in both the cis and trans configurations. Although the fact that these transition states actually connect $\mathbf{1}$ and $\mathbf{2}$ to $\mathbf{6}$ was not verified by IRC tracing, no other connections seem plausible. In TS($\mathbf{6} \rightarrow \mathbf{1}$) the ^{2}C–H$t$ distance was 1.201 Å and the ^{3}C–Ht distance 1.522 Å, where Ht is the migrating hydrogen. The corresponding distances in TS($\mathbf{6} \rightarrow \mathbf{2}$) were 1.199 Å and 1.526 Å, so the two transition states are quite similar. These interconversions are facile, as TS($\mathbf{6} \rightarrow \mathbf{1}$) (cis geometry) was 91.3 kJ mol^{-1} higher in energy than trans-$\mathbf{6}$ at the B3LYP/6-31G(d) level of theory, and 86.2 kJ mol^{-1} higher using B3LYP/6-31G(d,p) theory. This isomerization would actually occur from the cis ground state of $\mathbf{6}$, so the critical energy for reaction from that configuration would be 90.3 kJ mol^{-1}. TS($\mathbf{6} \rightarrow \mathbf{2}$) was located at 101.1 kJ mol^{-1}, providing a critical energy for that process. This energy is below the critical energy for TS($\mathbf{4} \rightarrow \mathbf{7}$)

(see below), so isomerization of $\mathbf{6}$ to $\mathbf{1}$ and $\mathbf{2}$ and vice versa is facile.

3.2.5. $6 \rightarrow 4$

The transition state for the methyl shift $\mathbf{6} \rightarrow \mathbf{4}$ that would interconvert branched and straight chain C1 ions was also characterized to elucidate the properties of such reactions (Fig. 14), even though results from ^{13}C labeling rule out the occurrence of that process [13]. TS($\mathbf{6} \rightarrow \mathbf{4}$) was 50.4 kJ mol^{-1} above the high point between $\mathbf{1}$ and $\mathbf{4}$, an energy high enough to make $\mathbf{6} \rightarrow \mathbf{4}$ noncompetitive with $\mathbf{1} \rightleftarrows \mathbf{2} \rightleftarrows \mathbf{3} \rightleftarrows \mathbf{4}$. However, the threshold for this reaction is comparable to that for dissociation of $\mathbf{1}$ to CH$_2$=CHCH=OH$^+$ + CH$_3^\cdot$, so the three-membered-ring–methyl shift $\mathbf{6} \rightarrow \mathbf{4}$ would be feasible in the absence of competing processes.

3.3. Conversion of C1 to C2 ions

The three-membered ring–methyl shift $\mathbf{4} \rightarrow \mathbf{7}$ was the lowest energy route found from C1 to C2 ions, validating previous suppositions [13,31] that this is the dominant step that converts C1 ions to C2 ions. This transition state (Fig. 15) is nearly symmetric, the distances from the methyl carbon to ^{1}C being 1.978 Å and that to ^{2}C 1.972 Å. TS($\mathbf{4} \rightarrow \mathbf{7}$) is 22.1 kJ mol^{-1}
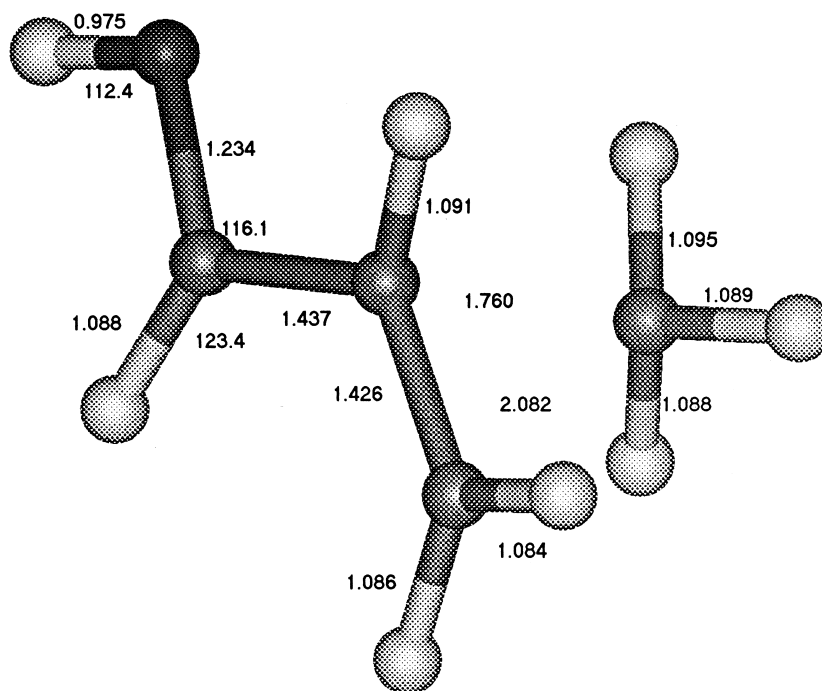
Fig. 14. Geometry for TS(**6 → 4**) obtained by DFT.

below $\Delta_f H(CH_3^.)$ + $\Delta_f H(CH_2=CHCHOH^+)$, predicting C1–C2 conversion substantially below that dissociation threshold. TS(**4 → 7**) was placed only 44.6 kJ mol^{-1} above ΔH_f of the C1 reactant **4** and 30.9 kJ mol^{-1} above the C2 product **7**, so **4 → 7** should be facile. Although this barrier is rather low, it is higher than the one of about 1 kJ mol^{-1} to the corresponding H shift $CH_2=CHCH_2OH^{+.}$ → $CH_2^.CH_2CH=OH^+$ [16]. Thus allylic and isomeric β-distonic ions are generally easily interconverted both by H and alkyl shifts.

The energy of the transition state for the four-membered-ring–methyl shift **6 → 7** (Fig. 16) was placed only 17.9 kJ mol^{-1} higher than **4 → 7** and only 4.2 kJ mol^{-1} below $CH_3^.$ + $CH_2=CHCH=OH^+$, so conversion of C1 to C2 ions might also occur by **6 → 7**. The $C_3H_5O^+$ portion of this ion was planar and the methyl group far from the other carbons (^{4}C–^{3}C 3.461 Å, ^{4}C–^{2}C 3.608 Å, ^{4}C–^{1}C 3.612 Å), so that transition state closely resembles a methyl-protonated acrolein ion–neutral complex. This picture is supported by overlap densities of merely 0.0065 and 0.0066 be-

tween the methyl carbon and C1 and C3, respectively, and charge and spin densities on the migrating methyl of 0.095 and 0.904, respectively. Binding energies of 12–13 kJ mol^{-1} in methyl-containing complexes have been obtained by ab initio means [40,41], so TS(**6 → 7**) is close enough to the dissociation threshold to be considered a complex. In previously characterized methyl-containing complexes [40,41] the methyls are parallel to their partners, whereas in TS(**6 → 7**) the methyl is perpendicular to its partner. This orientation might reduce the binding energy from the approximately 12 kJ mol^{-1} found for previous methyl-containing complexes to the 4 kJ mol^{-1} found for TS(**6 → 7**).

1,3-methyl shifts with inversion of configuration are allowed and those occurring with retention of configuration are forbidden [42] according to the Woodward–Hoffmann rules [43]. Consistent with this, the nearly perpendicular orientation of the methyl in TS(**6 → 7**) suggests that **6 → 7** occurs with inversion of the methyl configuration, despite the great distance between the methyl and the rest of the
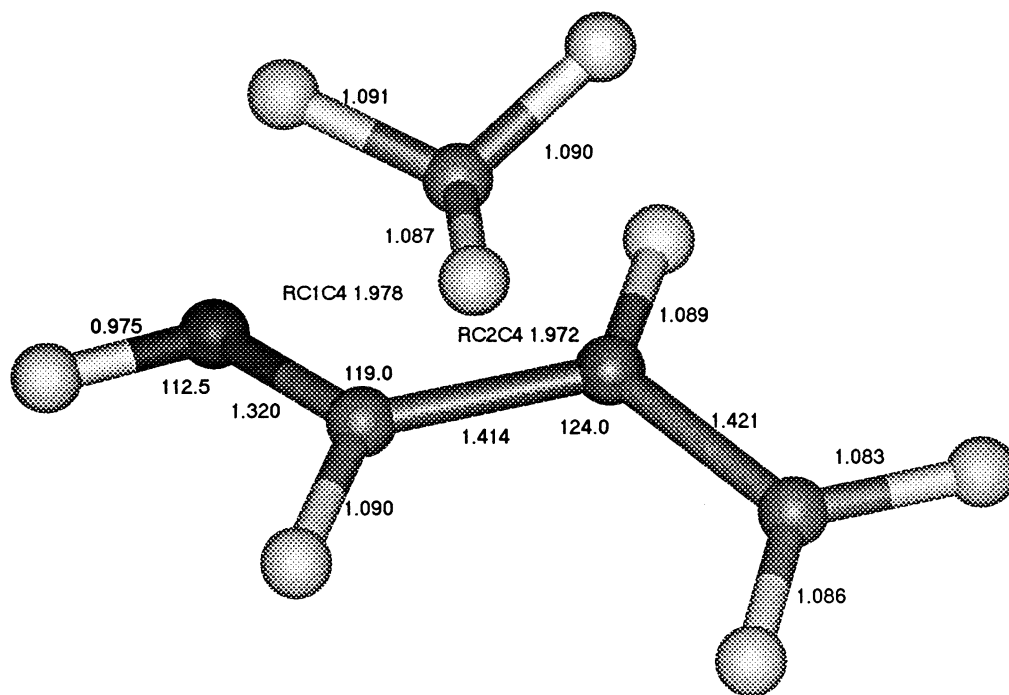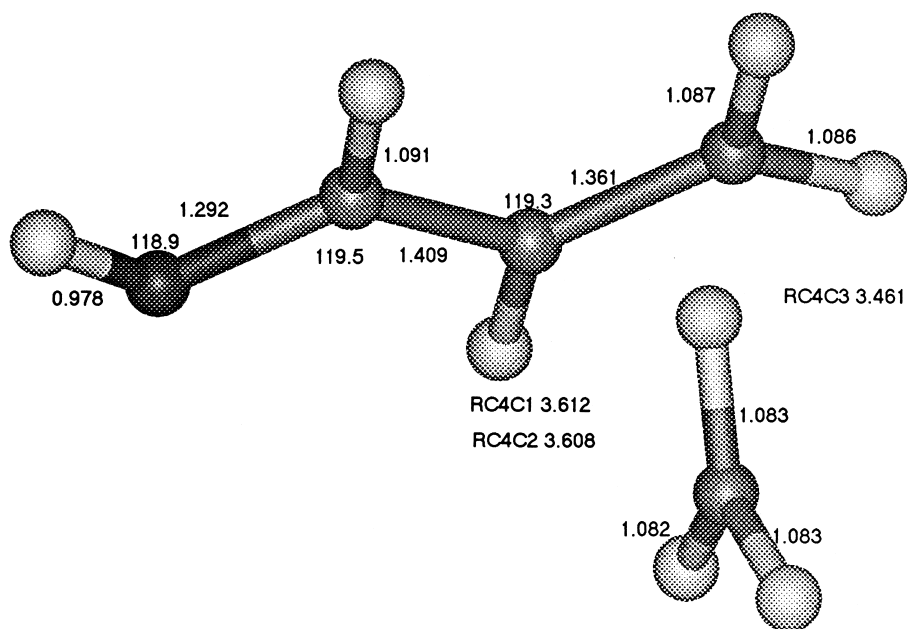
Fig. 15. Geometry for TS(**4 → 7**) obtained by DFT.

Fig. 16. Geometry for TS(**6 → 7**) obtained by DFT. Although it is not apparent in the figure, two of the hydrogens of the methyl essentially straddle the $^2C^3C$ bond with the third methyl hydrogen directed away from the $C_3H_5O^+$ partner (from methyl hydrogens, distances are: H^2C 3.250 Å, 3.270 Å and 4.652 Å, and H^3C distances are 3.023 Å, 3.428 Å, and 4.676 Å).

ion. This suggests that there are bonding interactions throughout this methyl migration, despite the low overlap C–C densities. We recently found that Woodward–Hoffmann restrictions operate in several isomerizations in gas phase ion chemistry to which their application was questionable [44–46].

Another possible pathway for converting C1 to C2 ions is that illustrated in Scheme 3. To determine whether this pathway is feasible, the bond between ^{2}C and ^{3}C in **2** was forced open in DFT theory. The energy rose steadily and surprisingly the oxygen shifted to ^{3}C to produce **7**, in contrast to the formation of **9** depicted in Scheme 3. The maximum energy at any point examined by this procedure was 179 kJ mol^{-1} above the DFT energy of **6**, but this was not the energy for a defined transition state. This point was about 20 kJ mol^{-1} higher in energy than the highest points in Figs. 1 and 2, so this reaction would not be expected to actually occur. As predicted, this reaction does not occur, as ^{13}C labeling has demonstrated that the oxygen never leaves ^{1}C in $C_4H_8O^{+\cdot}$ ions [13]. However, this does suggest that novel O shifts would occur in energized $C_nH_{2n}O^{+\cdot}$ ions in the absence of lower energy competing processes.

Acknowledgement

References

[1] H.E. Audier, G. Sozzi, Org. Mass Spectrom. 19 (1984) 150.
[2] H.E. Audier, A. Milliet, G. Sozzi, Org. Mass Spectrom. 19 (1984) 522.
[3] H.E. Audier, J.P. Denhez, P. Mourgues, Rapid Commun. Mass Spectrom. 3 (1989) 273.
[4] H. Schwarz, in J.F.J. Todd (Ed.), Advances in Mass Spectrometry, Wiley, New York, 1985, p. 13.
[5] G. Bouchoux, Mass Spectrom. Rev. 7 (1988) 1.
[6] G. Bouchoux, Mass Spectrom. Rev. 7 (1988) 203.
[7] D.J. McAdoo, C.E. Hudson, J. Mass Spectrom. 30 (1995) 492.
[8] D.J. McAdoo, Org. Mass Spectrom. 23 (1988) 350.
[9] H.E. Zimmerman, A. Zweig, J. Am. Chem. Soc. 83 (1961) 1196.
[10] C. Walling in P. de Mayo (Ed.), Molecular Rearrangements, Interscience, New York, 1963, Vol. 7, p. 407.
[11] N.F. Phelan, H.H. Jaffé, M. Orchin, J. Chem. Ed. 44 (1967) 626.
[12] D.J. McAdoo, C.E. Hudson, D.N. Witiak, Org. Mass Spectrom. 14 (1979) 350.
[13] C.E. Hudson, D.J. McAdoo, Org. Mass Spectrom. 20 (1985) 402.
[14] C.E. Hudson, D.J. McAdoo, Org. Mass Spectrom. 17 (1982) 366.
[15] C.E. Hudson, D.J. McAdoo, Tetrahedron 46 (1990) 331.
[16] G. Bouchoux, A. Luna, J. Tortajada, Int. J. Mass Spectrom. Ion Processes 167/168 (1997) 353.
[17] D.J. McAdoo, F.W. McLafferty, T.E. Parks, J. Am. Chem. Soc. 94 (1972) 1601.
[18] D.J. McAdoo, C.E. Hudson, F.W. McLafferty, T.E. Parks, Org. Mass Spectrom. 19 (1984) 353.
[19] L.L. Griffin, K. Holden, C.E. Hudson, D.J. McAdoo, Org. Mass Spectrom. 21 (1986) 175.
[20] P.H. Hemberger, J.C. Kleingeld, K. Levsen, N. Mainzer, A. Mandelbaum, N.M.M. Nibbering, H. Schwarz, R. Weber, A. Weisz, C. Wesdemiotis, J. Am. Chem. Soc. 102 (1980) 3736.
[21] G. Bouchoux, Y. Hoppilliard, Int. J. Mass Spectrom. Ion Processes 55 (1983) 47.
[22] D.J. McAdoo, C.E. Hudson, J.J. Zwinselman, N.M.M. Nibbering, J. Chem. Soc. Perkin Trans. II (1985) 1703.
[23] W.J. van der Hart, J. Am. Soc. Mass Spectrom. 10 (1999) 575.
[24] C.E. Hudson, D.J. McAdoo, Org. Mass Spectrom. 19 (1984) 1.
[25] R.D. Bowen, A.G. Harrison, Org. Mass Spectrom. 24 (1989) 525.
[26] G. Bouchoux, Y. Hoppilliard, R. Flammang, A. Maquestiau, P. Meyrant, Org. Mass Spectrom. 18 (1983) 340.
[27] D.J. McAdoo, C.E. Hudson, Org. Mass Spectrom. 18 (1983) 466.
[28] Y. Hoppilliard, G. Bouchoux, Org. Mass Spectrom. 17 (1982) 534.
[29] F.W. McLafferty, D.J. McAdoo, J.S. Smith, R. Kornfeld, J. Am. Chem. Soc. 93 (1971) 3720.
[30] D.J. McAdoo, D.N. Witiak, J. Chem. Soc. Perkin Trans. II (1981) 770.
[31] R.D. Bowen, A.G. Harrison, J. Chem. Soc. Perkin Trans. II (1989) 1483.
[32] J.C. Traeger, D.J. McAdoo, Int. J. Mass Spectrom. Ion Processes 68 (1986) 35.
[33] O. Wiest, K.N. Houk, Top. Curr. Chem. 183 (1996) 2.
[34] O. Wiest, J. Am. Chem. Soc. 119 (1997) 5713.
[35] M.J. Frisch et al., GAUSSIAN 92; Gaussian, Inc.: Pittsburgh, PA, 1992.
[36] A. Nicolaides, D.M. Smith, F. Jensen, L.J. Radom, J. Am. Chem. Soc. 119 (1997) 8083.
[37] A.P. Scott, L. Radom, J. Phys. Chem. 100 (1996) 16502.
[38] C. Gonzalez, H.B. Schlegel, J. Chem. Phys. 90 (1989) 2154.
[39] C. Gonzalez, H.B. Schlegel, J. Phys. Chem. 94 (1990) 5523.

[40] S. Olivella, A. Solé, D.J. McAdoo, L.L. Griffin, J. Am. Chem. Soc. 116 (1994) 11078.

[41] S. Olivella, A. Solé, D.J. McAdoo, L.L. Griffin, J. Am. Chem. Soc. 117 (1995) 2557.

[42] J.A. Berson, Acc. Chem. Res. 1 (1968) 152.

[43] R.B. Woodward, R. Hoffmann, Ang. Chem. 8 (1969) 781.

[44] C.E. Hudson, A.J. Alexander, D.J. McAdoo, Tetrahedron 54 (1998) 5065.

[45] C.E. Hudson, D.J. McAdoo, J. Am. Soc. Mass Spectrom. 9 (1998) 130.

[46] C.E. Hudson, D.J. McAdoo, J. Am. Soc. Mass Spectrom. 9 (1998) 138.